GCAGS JOURNAL
A Publication of the Gulf Coast Association of Geological Societies
www.gcags.org

Quantitative Modeling of Secondary Migration: Understanding the Origin of Natural Gas Charge of the Haynesville Formation in the Sabine Uplift Area of Louisiana and Texas

Lauri A. Burke

U.S. Geological Survey, MS 939 Box 25046 DFC, Denver, CO 80225–0046, U.S.A.

ABSTRACT

The Upper Jurassic (Kimmeridgian) mudstones of the Haynesville Formation in the Sabine Uplift, Louisiana and Texas, are widely considered to be a self-sourced natural gas reservoir; however, additional sources of gas may have charged the mudstones in the Louisiana portion of the uplift. Secondary migration of hydrocarbons into the Sabine Uplift from downdip, gas-generating Jurassic source rocks in the North Louisiana Salt Basin was quantitively modeled in this study. Jurassic source rocks include the Smackover, Haynesville, and Bossier Formations.

Thermodynamic equations of state were used to determine thermophysical properties of supercritical methane and water under reservoir conditions. A time-dependent derivation of Darcy's Law for pressure-driven laminar fluid flow through porous media was used to model secondary migration at reservoir conditions. This study indicates secondary migration requires approximately 100,000 yr for pore fluids to migrate through 1.0 km of carrier beds having representative petrophysical, fluid, and reservoir properties of the Haynesville Formation. As an example migration pathway, the distance from the middle of the North Louisiana Salt Basin to the center of the Sabine Uplift is approximately 96 mi (155 km). Given migration velocities over this distance, 15.5 m.y. is required for hydrocarbons to migrate from the North Louisiana Salt Basin and charge the Haynesville Formation in the Sabine Uplift. This study also indicates supercritical water is 6 times more thermally conductive than methane under reservoir conditions; however, the relatively small volumes of migrated water likely did not transfer sufficient heat for the metagenesis of methane. Based on this study, a component of natural gas charging the Haynesville Formation of the Sabine Uplift area can reasonably be explained by lateral migration and hydrodynamic flow from thermally mature Jurassic source rocks located in adjacent basins.

INTRODUCTION

Hydrocarbon migration is one of the least understood processes of petroleum system science (Hantschel and Kauerauf, 2009; Hac, 2021), as these processes are difficult to prove either experimentally or theoretically. Primary migration or expulsion out of thermally mature, organic-rich, low-permeability source rocks may occur due to several proposed mechanisms, described here, which are related to hydrodynamic flow driven by pressure differentials. Differential pressure gradients between the source rocks and surrounding strata may cause hydrodynamic flow toward lower pressured regions. These pressure differentials may arise from various mechanisms. Source rock compaction during burial may cause interstitial pore fluids to become overpressured with respect to surrounding rocks. Alternatively, kerogen maturation into hydrocarbons and thermal conversion of oil to thermogenic gas may cause overpressuring within the source rock. Additionally, microfractures may develop within the compacted, overpressured source rock which act as higher permeability conduits for primary hydrocarbon migration.

Secondary migration is the process in which hydrocarbons move through permeable carrier beds, fault zones, and fracture networks to form an accumulation and is less controversial than primary expulsion mechanisms (Schowalter, 1979; Hac, 2021). Fluid transport processes in petrophysics and petroleum engineering at wellbore scales and production timeframes are approached differently than secondary migration modeling for basin analysis and total petroleum systems that occur at basin scales over geologic timeframes (Fig. 1). Shale gas transport can be described by governing equations acting at molecular to wellbore magnitudes for fluid dynamics within the kerogen, low-permeability matrix, microfracture network, and formation (Javadpour et al., 2007; Wang and Reed, 2009; Ozkan et al.,

Manuscript received February 3, 2021; revised manuscript received April 21, 2021; manuscript accepted April 27, 2021.

GCAGS Journal, v. 10 (2021), p. 24–30.

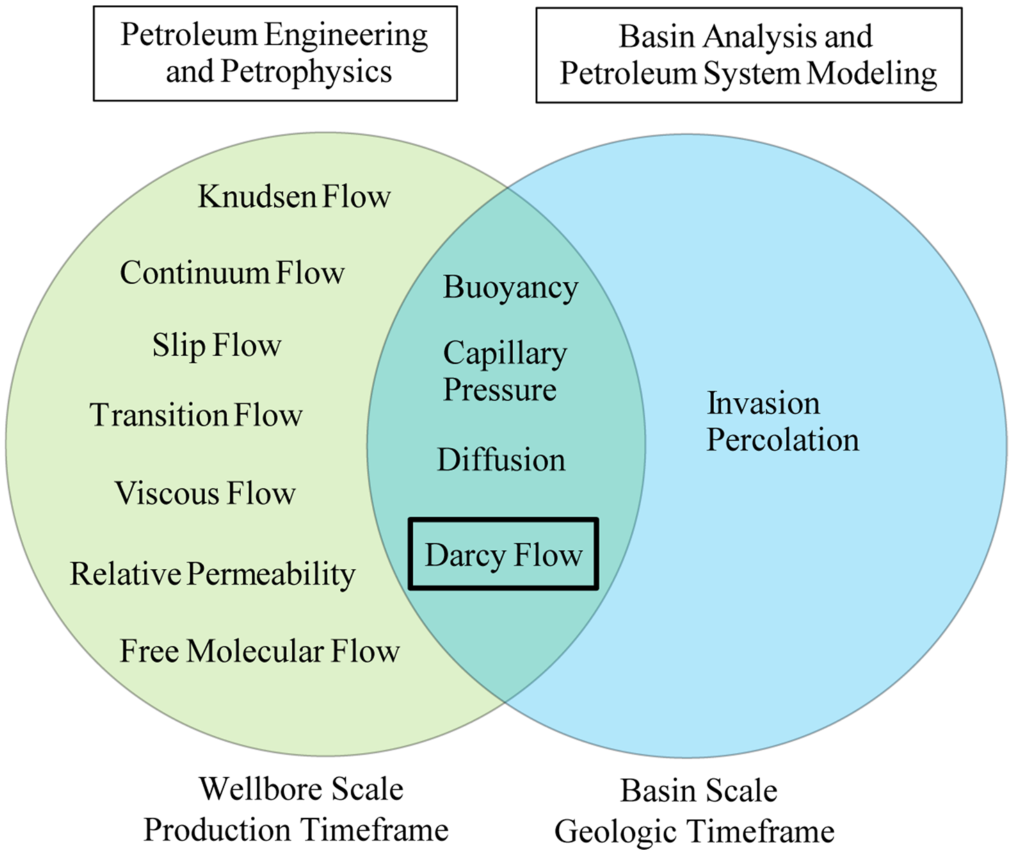

Figure 1. Novel Venn diagram of mathematical models describing fluid transport in petroleum engineering and petrophysics occuring at wellbore and reservoir scales over production timeframes (green circle) and models appropriate for secondary migration of hydrocarbons at basin scale over geologic timeframes (blue circle). This study of the Haynesville Formation quantifies secondary migration velocities within low-permeability source rock carrier beds using Darcy's Law of laminar flow through porous media.

2010; Wei et al., 2018). However, several input variables are required for fluid transport modeling at reservoir scales and production time horizons are irrelevant for flow modeling of secondary migration (Carruthers, 2003). The appropriate input variables for secondary migration include buoyancy, capillary pressure, Darcy flow, and percolation theory (Hunt, 1996; Hantschel and Kauerauf, 2009).

For this study of migration occurring within low-permeability carrier beds, Darcy flow is assumed to be an appropriate model for velocity calculations. For secondary migration occurring vertically across stratigraphic layers, a harmonic average of buoyancy and capillary forces would be appropriate to consider; however, velocities are assumed to be instantaneous. The objectives of this study were to quantify secondary migration velocities of dry gas, first with development of a general model encompassing substantial pressure and temperature ranges likely encountered in the sedimentary sequence, and secondly with a specific fluid flow model customized for reservoir properties of interest.

GEOLOGIC SETTING AND STRATIGRAPHY

Intervals within the Upper Jurassic (Kimmeridgian) Haynesville Formation are organic-rich carbonate mudstones deposited in a restricted basin setting during a global second-order sea level transgression (Wang and Hammes, 2010; Hammes et al., 2011) in which anoxic bottom water conditions were favorable for the preservation of fine-grained organic matter necessary for world-class source rocks. The productive trend of the Haynesville Formation shale gas reservoirs is delineated by the red shaded region along the Louisiana-Texas border in Figure 2 and includes the majority of the Sabine Uplift. Haynesville reservoirs range from 10,000–18,000 ft (3048–5486 m) in depth, exhibit high temperatures up to 430ºF (221ºC), and overpressure gradients from 0.70–0.95 psi/ft (15.8–21.5 kPa/m) (Wang et al., 2013) (Table 1).

According to recent assessments by the U.S. Geological Survey (USGS), the Haynesville Formation (Fig. 3) is estimated to contain undiscovered, technically recoverable resources of a mean of 1.1 billion barrels of oil, a mean of 195.8 trillion cubic feet of natural gas, and a mean of 0.9 billion barrels of natural gas liquids (Paxton et al., 2018), making this an important domestic resource.

Although the Haynesville Formation is widely considered to be a self-sourced natural gas reservoir (Hammes et al., 2011), there is potential for exogenous, overpressured hydrocarbons originating from thermally mature Jurassic source rocks, for example, in the adjacent North Louisiana Salt Basin, to provide an additional source of thermogenic gas to the Haynesville in the Sabine Uplift.

METHODOLOGY

Modern derivation for Darcy's Law (Whitaker, 1985) for laminar flow of a viscous, Newtonian fluid through porous media is a proportional relation between the pressure gradient over a distance, $\Delta P/L$; fluid viscosity, η; matrix permeability, κ; and pore throat cross sectional area, A, through which fluid passes. The Darcy flow rate, Q, is defined as:

$$Q = \frac{\kappa A}{\eta}\frac{\Delta P}{L}. \tag{1}$$

When this expression is solved in terms of velocity, Darcy flux is obtained. Darcy flux divided by porosity, ϕ, yields the interstitial pore velocity:

$$\vec{v} = \frac{\kappa \Delta P}{\eta \phi L} \tag{2}$$

as a function of rock and fluid properties as well as the pressure gradient within the carrier bed (see Table 2).

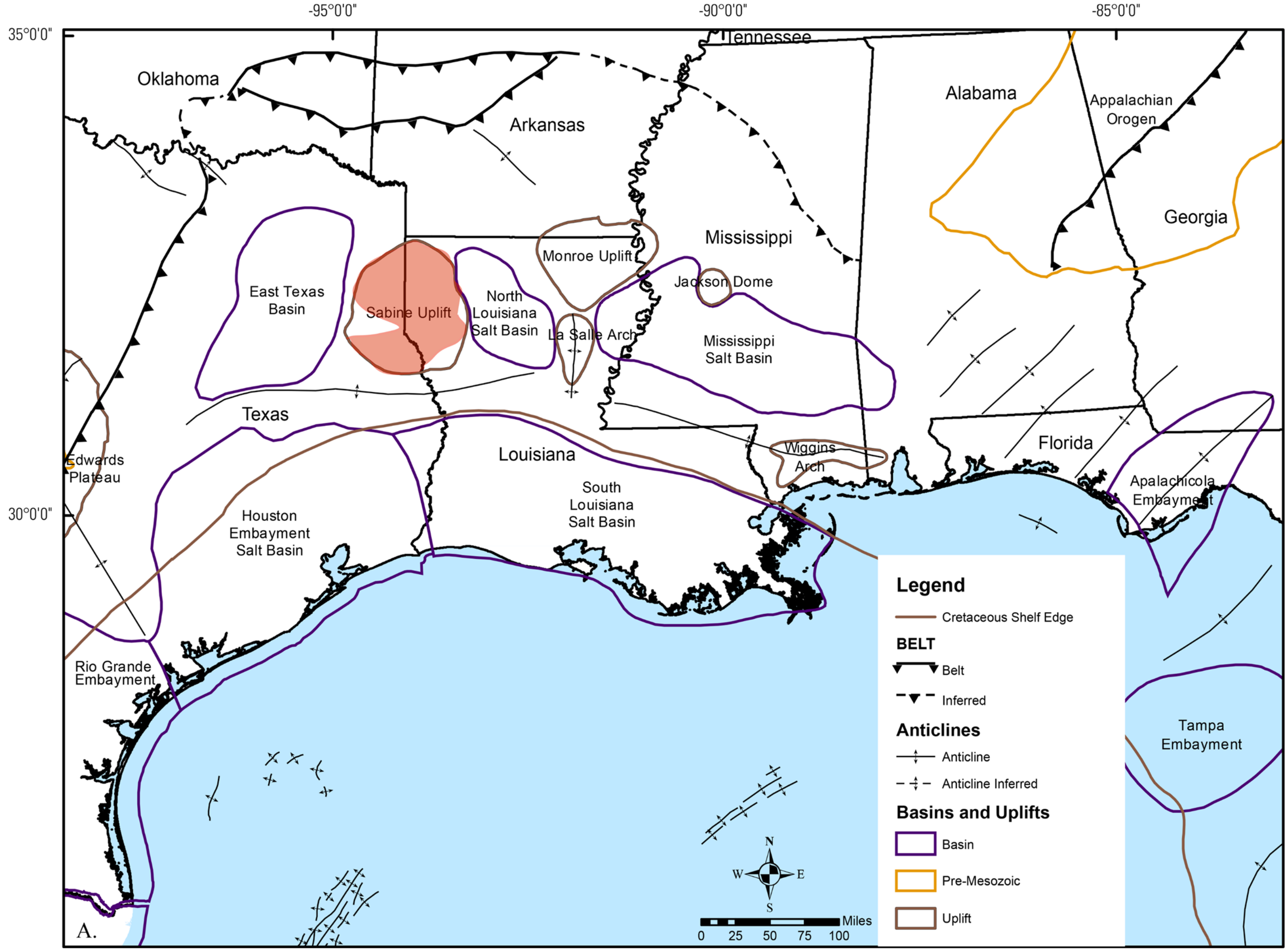

Figure 2. Index map of the northern Gulf of Mexico Basin showing major structural elements (modified after Ewing, 1991; Ewing and Lopez, 1991; Salvador et al., 1991) including basins, uplifts, anticlines, orogenic belts, and the Cretaceous shelf edge (Galloway, 2008). Productive trend of the Haynesville Formation is approximated by the red shaded area (after Hammes et al., 2011).

Table 1. Summary of representative reservoir conditions and formation properties for the Haynesville Formation (after Wang et al., 2013).

Property	**Range (English)**	**Average (English)**	**Range (metric)**	**Average (metric)**
Depth	10,000–18,000 ft	14,000 ft	3048–5486 m	4267 m
Reservoir pressure	8000–17,000 psi	12,500 psi	55.2–117.2 MPa	86.2 MPa
Pressure gradient	0.70–0.95 psi/ft	0.83 psi/ft	15.8–21.5 kPa/m	18.8 kPa/m
Temperature	260–430ºF	345ºF	127–221ºC	174ºC
Thermal maturity	1.25–2.3 Ro	1.8 Ro	1.25–2.3 Ro	1.8 Ro
Total organic carbon	0.5–7.0%	3.80%	0.5–7.0%	3.80%
Porosity	3–14%	9%	3–14%	9%
Permeability	400 nD	400 nD	3.948×10^{-19} m^2	3.948×10^{-19} m^2

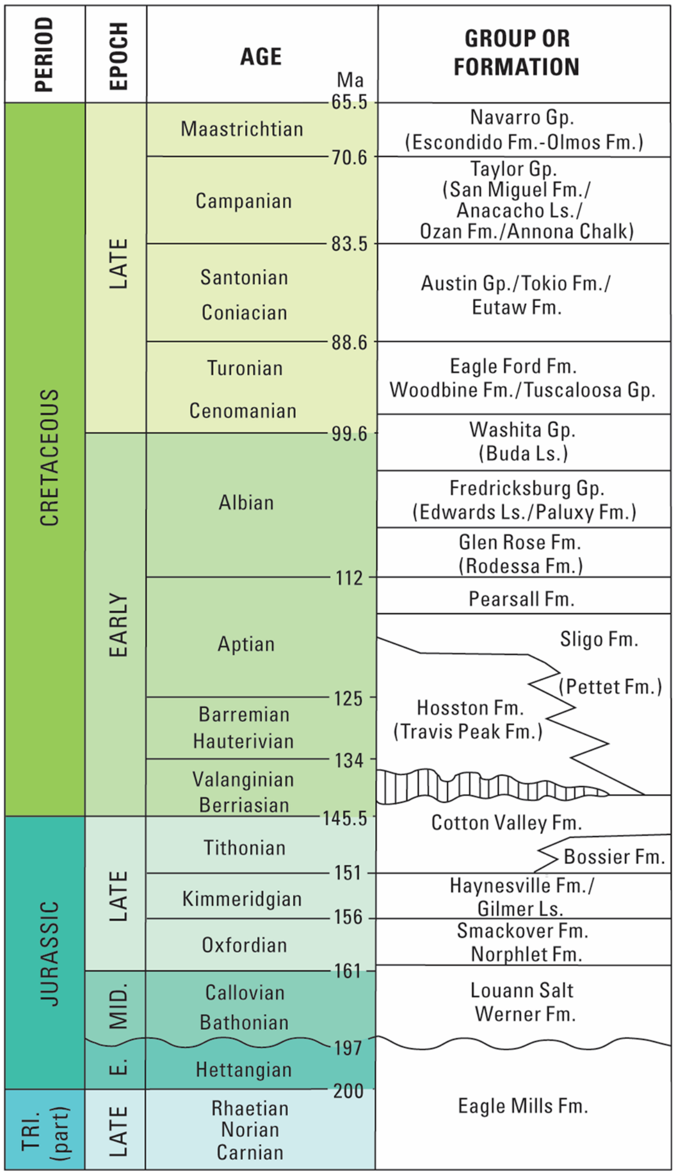

Figure 3. Generalized stratigraphic column of onshore Gulf Coast strata showing Upper Jurassic Smackover Haynesville, and Bossier Formations (from Dubiel et al., 2011, courtesy of the U.S. Geological Survey).

Table 2. Symbols used in equations.

A	Cross sectional area
κ	Matrix permeability
L	Lateral distance
P	Pressure
v	Interstitial pore velocity
ϕ	Fractional porosity
η	Fluid viscosity
τ	Timeframe
Q	Darcy fluid flow rate
Δ	Gradient differential

Solving in terms of timeframe, τ_D, the Darcy flux of a viscous fluid through a porous media across a lateral distance, L, is expressed as:

$$\tau_D = \frac{\eta\phi L^2}{\kappa\Delta P}. \tag{3}$$

Calculations of migration velocities and timescales rely upon several physical models which include conservation of energy (i.e. constitutive equations from thermodynamics), conservation of momentum (i.e. Navier-Stokes general solutions for Darcy's Law), and conservation of mass (i.e., fluid transport in porous media). Modeling begins with calculating thermophysical properties of supercritical pore fluids (described in the next section) for reservoir and temperature conditions representative of the Haynesville Formation. These thermophysical fluid properties are then input into the time-depended form of Darcy's Law. Finally, rock properties of the formation are used to constrain the velocity and timescales of fluid migration.

THERMOPHYSICAL PROPERTIES AND THERMAL CONDUCTIVITY

Thermophysical properties of pore fluids under a wide range of reservoir conditions likely encountered in the sedimentary sequence were used for modeling secondary migration. Density and viscosity of supercritical methane (Figs. 4A and 4B) for pressures from 0 to 29,000 psi (0 to 200 MPa) at isothermal conditions of 350ºF (177ºC) were calculated from the Reference Fluid Thermodynamic and Transport Properties Database (NIST, 2019), based on equations of state from Setzmann and Wagner (1991) and thermophysical fluid properties (Younglove and Ely, 1987; Richter and McLinden, 2014). Density increases logarithmically as a function of pressure, while viscosity increases almost linearly as a function of pressure. Compressional-wave velocity of supercritical methane linearly increases as a function of pressure (Fig. 4C). Fluid compressibility (Fig. 4D) as a function of pressure was calculated from the inverse of fluid bulk modulus based on the methodology from Burke (2011).

Thermal conductivities of methane and water (Figs. 4E and 4F) over the temperature range of 0–450ºF (-10–232ºC) at reservoir pressure of 12,500 psi (86.2 MPa) were obtained from NIST (2019) to investigate if migrated water could have introduced sufficient heat for the metagenesis of dry gas observed in Haynesville accumulations. Water increases in thermal conductivity as a function of temperature, attains a maximum at 325ºF (163ºC), then decreases in thermal conductivity as temperature continues to rise. Methane, however, decreases in thermal conductivity as temperature increases. Observations indicate that supercritical water is 6 times more thermally conductive than methane at these reservoir conditions.

MODELING RESULTS AND INTERPRETATION

Modeling results for pressure-driven fluid transport (Fig. 4) were calculated for a general case that covered a substantial range of rock and fluid properties likely encountered in sedimentary basins. For the general case, pressure differentials ranged from 0 to 29,000 psi (0 to 200 MPa). Fluid transport was calculated through homogeneous isotropic porous media exhibiting porosities ranging from 0 to 99 percent. Migration velocities for permeabilities ranging over 12 orders of magnitude from 1 Darcy (D) down to 1 pD (1×10^{-12} D) were calculated. The general case provides timescales for pore fluid migration through 1.0 km of strata. Given the broad range of pressures and rock properties that are represented by this model, results are applicable for an array of reservoirs exhibiting 350 ± 50ºF reservoir temperature. Deviation from this temperature range would alter the fluid properties and resultant velocities.

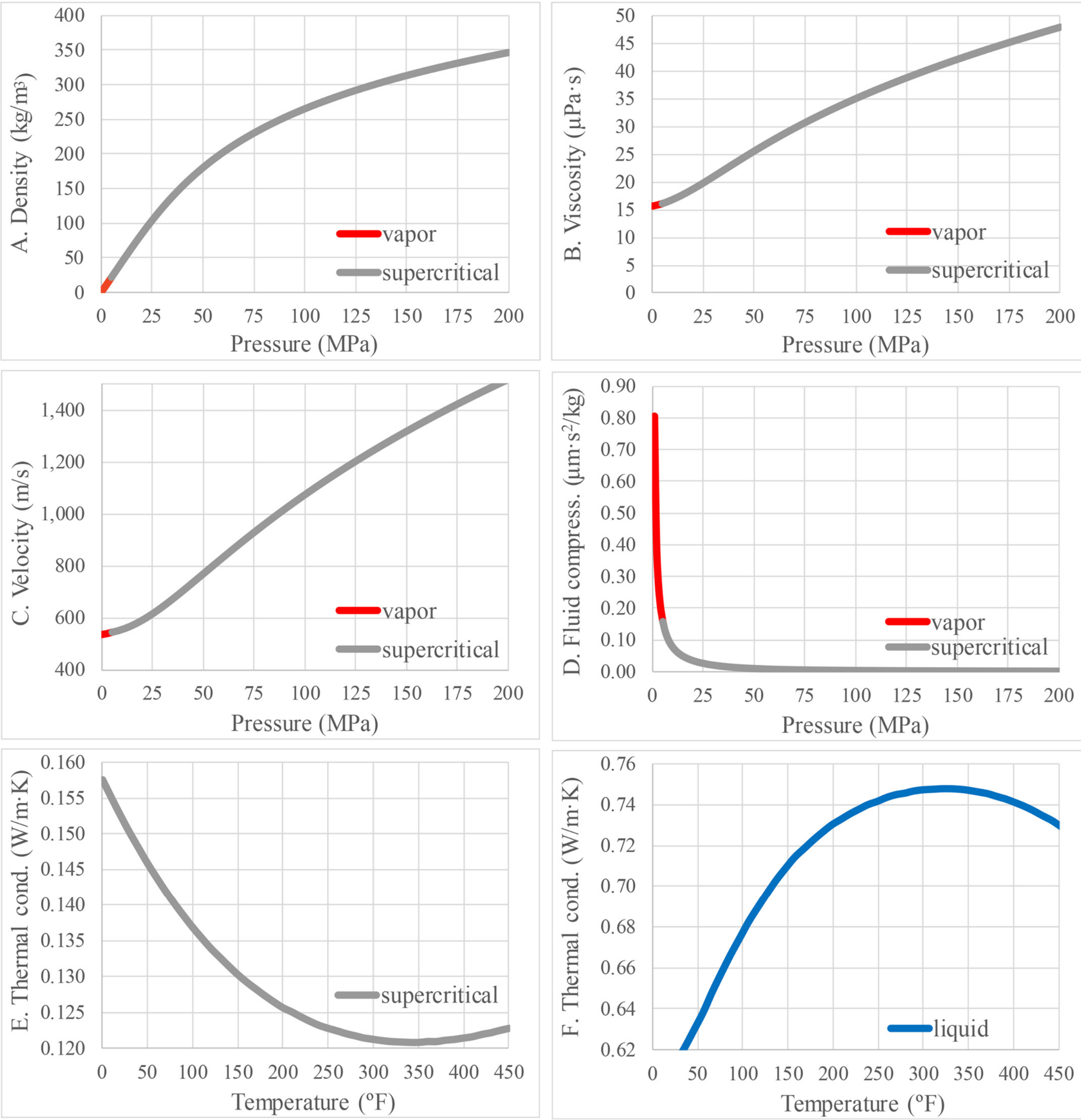

Figure 4. (A–D) Thermophysical properties of supercritical methane over a wide range of reservoir pressures likely encountered in the sedimentary sequence. Thermal conductivities (cond.) of supercritical methane (E) and water (F) over a wide range of temperature conditions likely encountered in sedimentary basins. Fluid compressibility (compress.) was calculated based on the methodology by Burke (2011); other parameters were obtained from NIST (2019).

For this specific modeling case, representative subsurface properties for the Haynesville Formation were compiled and summarized in Table 1 (after Wang et al., 2013). Representative Haynesville Formation properties, which exhibit an average of 9% porosity and 400 nD (1×10^{-9} D) permeability, are interpreted on the migration model (Fig. 5, blue polygon). These findings indicate, for this specific case, secondary migration requires approximately 1×10^{5} yr (100,000 yr) for natural gas to migrate laterally through 1.0 km of carrier beds exhibiting representative petrophysical, fluid, and reservoir properties of the Haynesville Formation.

As an example migration pathway, the distance from the middle of the North Louisiana Salt Basin to the center of the Sabine Uplift is approximately 96 mi (155 km). Given these parameters, 15.5 m.y. is required for dry gas migration from the thermally mature Haynesville Formation in North Louisiana Salt Basin

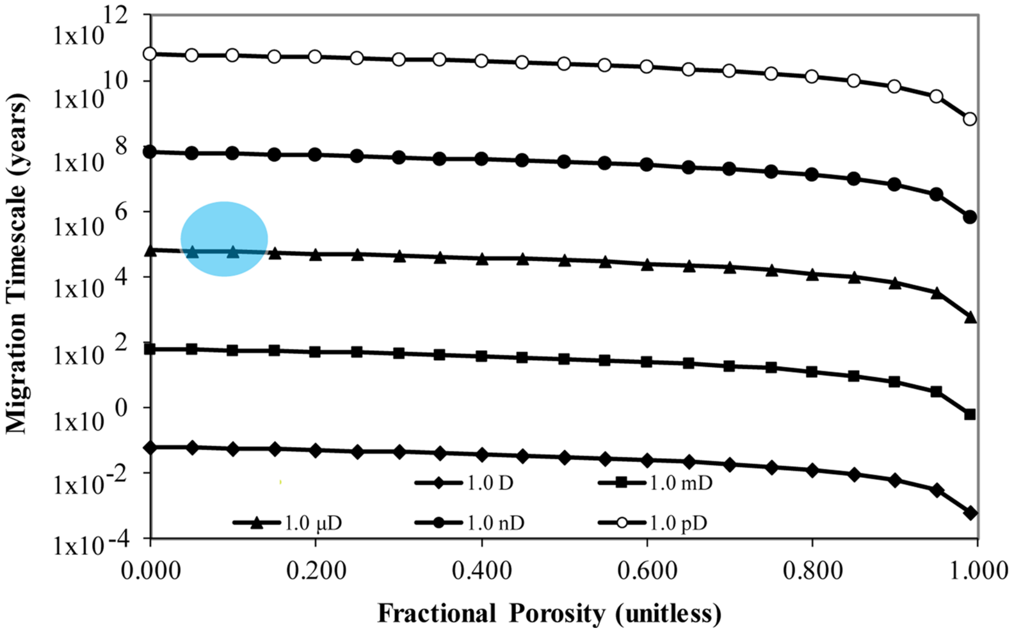

Figure 5. Secondary migration quantitative modeling results. The general case provides timescales for pore fluid migration through 1.0 km of strata exhibiting a substantial range of porosity and permeability, which makes this model applicable for a wide array of reservoirs encountered in the sedimentary sequence. The specific modeled case (blue polygon) indicates secondary migration through 1.0 km of carrier beds having representative petrophysical, fluid, and reservoir properties of the Upper Jurassic Haynesville Formation requires on the order of 1×10^5 yr (100,000 yr).

(Torsch, 2012) to charge the Haynesville in the Sabine Uplift. Although 15.5 m.y. is beyond the production timeframe of moving hydrocarbons from the reservoir into the wellbore, it is well within the geologic timeframe to charge a reservoir.

Sensitivity analysis revealed porosity and permeability are the primary factors influencing migration velocities. The presence of higher permeability conduits, such as fracture and fault zones, can be incorporated into the model by adjusting porosity and permeability values. Open fractures or matrix with higher porosity and permeability enable pore fluids to migrate at faster velocities. Sensitivity analysis revealed various methane-water saturations impact fluid compressibility in a negligible way relative to million-year timescales. Saturation impacts fluid viscosity linearly and is also below the order-of-magnitude resolution of this technique. Results of this study indicate that supercritical water is 6 times more thermally conductive than methane under these reservoir conditions; however, the relatively small volumes of migrated water during primary generation and expulsion (Wang et al., 2013) likely did not transfer sufficient heat for the metagenesis of dry gas. Based on these results, a component of natural gas that charges the Haynesville Formation in the Sabine Uplift area can be reasonably explained by lateral migration and hydodynamic flow from mature Jurassic source rock, for example, from the adjacent North Louisiana Salt Basin.

CONCLUSIONS

Quantitative migration velocities were modeled using a time-dependent form of Darcy's Law for laminar fluid flow through porous media over a substantial range of pressure conditions and rock properties likely encountered in the sedimentary sequence. This model to quantify secondary migration is applicable for a wide array of reservoirs. Modeling results indicate 15.5 m.y. are required for secondary migration of hydrocarbons through carrier beds having representative petrophysical, fluid, and reservoir properties of the Haynesville Formation. This time horizon is appropriate for secondary migration of hydrocarbons at basin scales over geologic timeframes. Accordingly, reservoir charge of the Haynesville Formation may be reasonably explained, in part, by secondary migration of hydrocarbons originating from thermally mature Jurassic source rock within an adjacent basin, for example, the North Louisiana Salt Basin.

ACKNOWLEDGMENTS

The author acknowledges the Gulf Coast Association of Geological Societies for the opportunity to present this work and the U.S. Geological Survey (USGS) Gulf Coast Petroleum Systems Team members. Technical reviews of the manuscript were conducted by Justin Birdwell, Sarah Gelman, Sam Heller, Julie Herrick, Kristen Marra, Stanley Paxton, Ofori Pearson, Janet Pitman, Chilisa Shorten, Janet Slate, and Katherine Whidden. This research was funded by the USGS Energy Resources Program.

REFERENCES CITED

Burke, L. A., 2011, Carbon dioxide fluid-flow modeling and injectivity calculations: U.S. Geological Survey Scientific Investigations Report 2011–5083, 16 p., <https://pubs.usgs.gov/sir/2011/5083>.

Carruthers, D. J., 2003, Modeling of secondary petroleum migration using invasion percolation techniques, *in* S. Duppenbecker and R. Marzi, eds., Multidimensional basin modeling: American Association of Petroleum Geologists Datapages Discovery Series 7, Tulsa, Oklahoma, p. 21–37.

Dubiel, R. F., P. D. Warwick, S. Swanson, L. A. Burke, L. R. H. Biewick, R. R. Charpentier, J. L. Coleman, T. A. Cook, K. Dennen, C. Doolan, C. Enomoto, P. C. Hackley, A. W. Karlsen, T. R. Klett, S. A. Kinney, M. D. Lewan, M. Merrill, K. M. Pearson, O. N. Pearson, J. K. Pitman, R. M. Pollastro, E. L. Rowan, C. J. Schenk, and B. Valentine, 2011, Assessment of undiscovered oil and gas resources in Jurassic and Cretaceous strata of the Gulf Coast, 2010: U.S. Geological Survey Fact Sheet 2011–3020, 4 p., <https://pubs.usgs.gov/fs/2011/3020/pdf/FS11-3020.pdf>.

Ewing, T. E., 1991, Structural framework, *in* A. Salvador, ed., The geology of North America, v. J: The Gulf of Mexico Basin: Geological Society of America, Boulder, Colorado, p. 31–52, <https://doi.org/10.1130/DNAG-GNA-J>.

Ewing, T. E., and R. F. Lopez, 1991, Principal structural features, Gulf of Mexico Basin, *in* A. Salvador, ed., The geology of North America, v. J: The Gulf of Mexico Basin: Geological Society of America, Boulder, Colorado, pl. 2, <https://doi.org/10.1130/DNAG-GNA-J>.

Galloway, W. E., 2008, Depositional evolution of the Gulf of Mexico sedimentary basin, *in* A. D. Miall, ed., Sedimentary basins of the world, v. 5: The sedimentary basins of the United States and Canada: Elsevier, Amsterdam, Netherlands, p. 505–549, <https://doi.org/10.1016/S1874-5997(08)00015-4>.

Huc, A. Y., 2021, Migration of hydrocarbons, *in* R. Sorkhabi, ed., Encyclopedia of petroleum geoscience: Springer, Cham, Switzerland, Encyclopedia of Earth Sciences Series, <https://doi.org/10.1007/978-3-319-02330-4_80-1>.

Hammes, U., H. S. Hamlin, and T. E. Ewing, 2011, Geologic analysis of the Upper Jurassic Haynesville Shale in East Texas and West Louisiana: American Association of Petroleum Geologists Bulletin, v. 95, p. 1643–1666, <https://doi.org/10.1306/02141110128>.

Hantschel, T., and A. I. Kauerauf, 2009, Fundamentals of basin and petroleum systems modeling: Springer, New York, 486 p., <https://doi.org/10.1007/978-3-540-72318-9>.

Hunt, J. M., 1996, Petroleum geochemistry and geology, 2nd. ed.: W. H. Freeman, New York, 743 p.

Javadpour, F., D. Fisher, and M. Unsworth, 2007, Nanoscale gas flow in shale gas sediments: Journal of Canadian Petroleum Technology, v. 46, Paper PETSOC–07–10–06, <https://doi.org/10.2118/07-10-06>.

NIST, 2019, National Institute of Standards and Technology Reference Fluid Thermodynamic and Transport Properties Database (REFPROP version 7): U.S. Department of Commerce, Gaithersburg, Maryland, <https://www.nist.gov/srd/refprop>.

Ozkan, E., R. S. Raghavan, and O. G. Apaydin, 2010, Modeling of fluid transfer from shale matrix to fracture network: Society of Petroleum Engineers Paper 134830, Richardson, Texas, 18 p., <https://doi.org/10.2118/134830-MS>.

Paxton, S. T., J. K. Pitman, S. A. Kinney, N. J. Gianoutsos, O. N. Pearson, K. J. Whidden, R. F. Dubiel, C. J. Schenk, L. A. Burke, T. R. Klett, H. M. Leathers-Miller, T. J. Mercier, S. S. Haines, B. A. Varela, P. A. Le, T. M. Finn, S. B. Gaswirth, S. J. Hawkins, K. R. Marra, and M. E. Tennyson, 2018, U.S. Geological Survey input-data forms for the assessment of the Upper Jurassic Haynesville Formation, U.S. Gulf Coast, 2016: U.S. Geological Survey Open-File Report 2018–1130, 62 p., <https://doi.org/10.3133/ofr20181130>.

Richter, M., and M. O. McLinden, 2014, Vapor-phase (p,ρ,T,x) behavior and virial coefficients for the (methane + propane) system: Journal of Chemical Engineering Data, v. 59, p. 4151–4164, <http://doi.org/10.1021/je500792x>.

Salvador, A., R. B. William, R. L. Jose, and C. Cordova, 1991, Physiography and bathymetry, *in* A. Salvador, ed., The geology of North America, v. J: The Gulf of Mexico Basin: Geological Society of America, Boulder, Colorado, pl. 1, <https://doi.org/10.1130/DNAG-GNA-J>.

Schowalter, T. T., 1979, Mechanics of secondary hydrocarbon migration and entrapment: American Association of Petroleum Geologists Bulletin, v. 63, p. 723–760, <http://www.searchanddiscovery.com/documents/97018/mechan.htm>.

Setzmann, U., and W. Wagner, 1991, A new equation of state and tables of thermodynamic properties for methane covering the range from the melting line to 625 K at pressures up to 1000 MPa: Journal of Physical Chemistry Reference Data, v. 20, p. 1061–1155, <https://doi.org/10.1063/1.555898>.

Torsch, W. C., 2012, Thermal and pore pressure history of the Haynesville Shale in North Louisiana: A numerical study of hydrocarbon generation, overpressure, and natural hydraulic fractures: Master's Thesis, Louisiana State University, Baton Rouge, Louisiana, 82 p.

Wang, F. P., and U. Hammes, 2010, Effects of petrophysical factors on Haynesville fluid flow and production: World Oil, v. 231, p. D79–D82.

Wang, F. P., and R. M. Reed, 2009, Pore networks and fluid flow in gas shales: Society of Petroleum Engineers Paper 124253, Richardson, Texas, 8 p., <https://doi.org/10.2118/124253-MS>.

Wang, F. P., U. Hammes, and L. Qinghui, 2013, Overview of Haynesville shale properties and production, in U. Hammes and J. Gale, eds., Geology of the Haynesville gas shale in East Texas and West Louisiana: American Association of Petroleum Geologists Memoir 105, Tulsa, Oklahoma, p. 155–177, <https://doi.org/10.1306/13441848M1053527>.

Wei, M., J. Lui, D. Elsworth, and E. Wang, 2018, Triple-porosity modelling for the simulation of multiscale flow mechanisms in shale reservoirs: Geofluids, 2018 vol., Article 6948726, 11 p., <https://doi.org/10.1155/2018/6948726>.

Whitaker, S., 1985, Flow in porous media I: A theoretical derivation of Darcy's law: Transport in Porous Media, v. 1, p. 3–25, <https://doi.org/10.1007/BF01036523>.

Younglove, B. A., and J. F. Ely, 1987, Thermophysical properties of fluids II: Methane, ethane, propane, isobutane, and normal butane: Journal of Physical and Chemical Reference Data, v. 16, p. 577–799, <https://doi.org/10.1063/1.555785>.